Evaluation of the lightning strike risk applied to particular site located in the French pyrenees

Charly Sigogne, Thierry Reess, Antoine Silvestre de Ferron

Evaluation of the lightning strike risk applied to particular site located in the French pyrenees

Charly Sigogne[1, *], Thierry Reess[2], Antoine De Ferron[2]

[1] ABB Pole Foudre, Bagnères de Bigorre, France
[2] Laboratoire des Sciences de l'Ingénieur Appliquées à la Mécanique et au génie Electrique,
Université de Pau & pays de l'Adour, France

* Corresponding author: charly.sigogne@fr.abb.com (Charly Sigogne)

Abstract

In the domain of lightning protection, the vulnerability of structures to lightning is commonly estimated by using the rolling sphere method. This is an electrogeometric model (EGM) and consists in placing over the structure an imaginary sphere of a radius which depends on the estimated peak current of the lightning flash return stroke. In this way all the surface contact points are considered to require protection, whilst the remaining unaffected volume is assumed to be fully protected. In the present work, we propose a novel method allowing the evaluation of the lightning impact probability over a structure. The new approach is applied in the case of the Observatory of the Pic du Midi de Bigorre, in the South of France, where a lightning station is installed. Firstly, an analysis of the lightning characteristics observed at this site is based on existing lightning data. Secondly the new method, based on a 3-D application of the electrogeometric model, is used to provide the probability for each point of the structure to be hit by a downward flash. Finally, the percentage of upward flashes is estimated and coupled with the probabilities for downward flashes to obtain the overall probabilities for the structure.

Keywords: Lightning protection, impact probabilities, 3D electrogeometric model.

1. Introduction

The electrogeometric model (EGM) and the rolling sphere method (RSM) associated with it are currently recommended for the implementation and design of protective devices against lightning, especially by the standard IEC62305-1. This model allows highlighting the areas likely to be struck by lightning [1–3]. The model however is based solely on experimental observations and ignores the influence of physical characteristics of soil, aerosols, altitude and other climatic parameters [4]. These simplifications often lead to erroneous conclusions. Indeed, the electric charges induced by the thundercloud to the ground surface, where electric field maxima are noticeable, cause the appearance of upward leaders [5]. This phenomenon becomes more important when the site to be protected is placed at high altitude [6]. It is therefore necessary to change the EGM and the RSM by introducing more realistic physical parameters.

The EGM is applicable only in the case of negative downward flashes and specifies if an area is likely to be struck by lightning or not [2, 3]. The purpose of this paper is to quantify the probability of lightning on these areas. These probabilities will then be coupled with an analysis of detection network data to integrate parameters such as current distribution, the multiplicity or the upward flashes percentage. Before being used, the new model must be validated by comparing its predictions to available experimental results. Several types of experiments allow studying the lightning capture at various scales: the discharges in high voltage laboratory, the triggered lightning or studies under natural conditions. The laboratory tests consider only part of the phenomenon and remain confined to a small scale when compared with real discharges. For example, the triggered lightning increases the probability of lightning, but the upward leaders are removed [7]. It is clear that only a study of the real natural phenomena allows understanding all the parameters and their variability.

However, the number of natural lightning flashes can be very low and therefore may limit the amount of useful data. Consequently, we propose to validate our method in natural conditions in a place often stricken by lightning and where a complex building exists having a rather limited extend. In France, the probability of lightning is generally low. However a global analysis of data provided by METEORAGE, the operator of the French national lightning locating system, has pointed out an interesting site at the Pic du Midi located in the Pyrenees (south of France) situated at a high altitude i.e., the top of the mountain has an elevation of 3,000 m [8]. This site is occupied by an astronomical observatory, the "Télé-Diffusion de France" (TDF) 100 m high broadcast antenna and other multi-purpose buildings nearby (Fig. 1). The place is also a major spot for tourism.

Related to the present work and in order to evaluate its efficiency, a 5 m high testing lightning rod was installed on the east side of the site on a tower located at approximately 150 m far from the TDF antenna. The lightning rod is attached to an experimental platform: the "Differential Image Motion Monitor" (DIMM) platform.
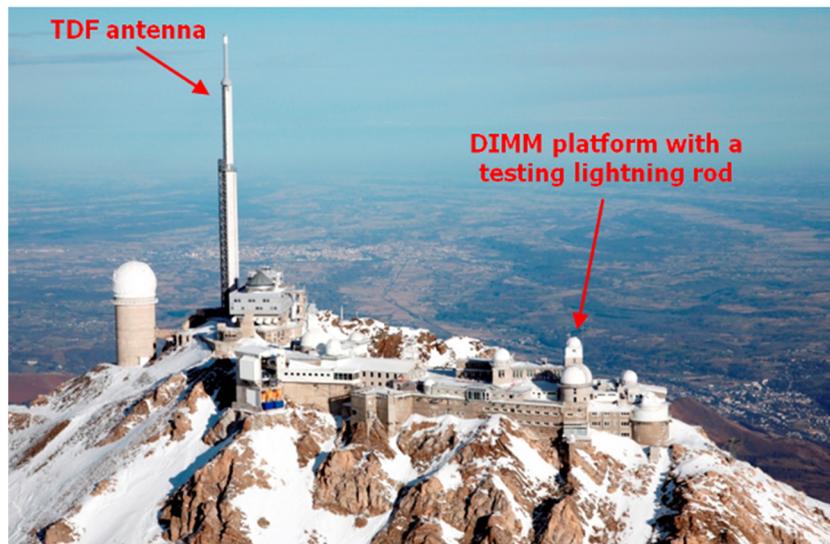

Fig. 1. Photography of the top of the Pic du Midi, with the tall TDF antenna and the testing lightning rod.

2.　Analysis of lightning detection network data

Before calculating impact probabilities, several parameters must be known concerning the lightning activity at the site. Parameters such as the lightning density, the multiplicity of strokes per flash, the current distribution or an estimation of the proportion of upward flashes, can all be obtained from an analysis of the lightning detection network data.

2.1 Strokes localization around the Pic du Midi

In France, the lightning detection network, managed by the company Météorage, was upgraded in 2009 [9]. The Pic du Midi is well situated inside the network and consequently the number and the quality of lightning data is very consistent. Fig. 2 presents a photo of the region, covering approximately 16 km^2 and centered on the Pic du Midi. The cloud-to-ground strokes collected by Météorage during four years of systematic study are shown as yellow crosses and it is clear that there is a large concentration around the top of the mountain. If only strokes situated at a distance smaller than 2 km around the Pic du Midi are considered, 77% of them are concentrated inside the highlighted 500 m radius circle of Fig. 2. Therefore, only cloud-to-ground strokes inside this circle are considered in this paper. Within this radius, all strokes are assumed to strike the Pic du Midi.

To obtain the average number of strokes per year, this data provided by the lightning detection network has been used and analyzed. The annual average of strokes per year is 144. This value will be used as input parameter to calculate the probabilities of lightning impact on the site of the Pic du Midi.
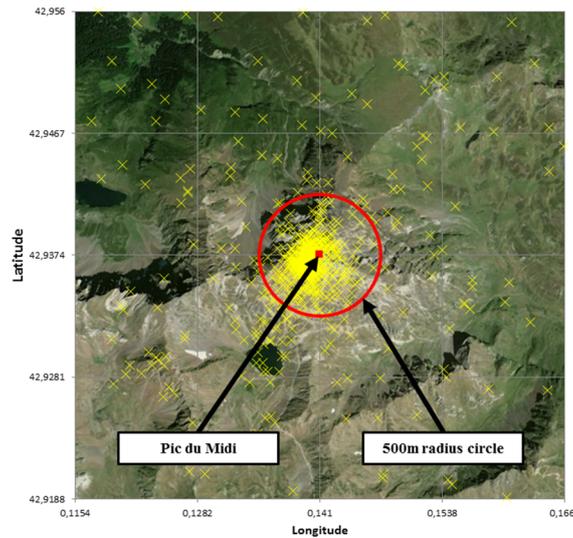
Fig. 2. Localization of strokes (crosses) around the Pic du Midi. The circle highlighted has 500 m radius.

2.2 Multiplicity analysis

The multiplicity analysis aims to determine the number of strokes per flash. The lightning detection network performance has a large influence on the multiplicity value [10]. In particular, strikes having low amplitude are very difficult to be detected by the network. Apart from this, the multiplicity calculation can also be affected by the fact that intra-cloud strokes are usually wrongly classified as cloud-to-ground strokes.

To estimate the multiplicity and to assign strokes for a given flash, Météorage applies an algorithm commonly used by lightning detection networks [11]. This algorithm assigns strokes to a given flash if time between two consecutive strokes is less than 500 ms, at a distance less than 10 km and if the total flash duration is less than 1 s. In such conditions the network can provide the strokes position in a flash and with this information it is usually possible to calculate the multiplicity. However, as the distance between strokes in a given flash can be up to 10 km, part of strokes is inside the 500 m radius circle around the Pic du Midi while the others well out of the circle. Consequently, it is necessary to recalculate the multiplicity with the same temporal criteria, but only using the strokes inside the 500 m radius.

Applying the method described above, flashes can be grouped related to their number of strokes as in Fig. 3, and the average multiplicity can be thus estimated. Considering only negative cloud-to-ground strokes in a 500 m radius, the average multiplicity is found to be about 4.36 strokes per flash. This value is in good agreement with that of 4.74, presented by Diendorfer *et al*. [12] in relation to the Gaisberg tower, a site having a similar topography to that of the Pic du Midi.

Fig. 3 shows that some flashes are composed from a large number of strokes i.e., more than 15 strokes per flash. According to Météorage, these discharges are probably parts of upward flashes, with many current pulses which could be detected as different strokes by the network.
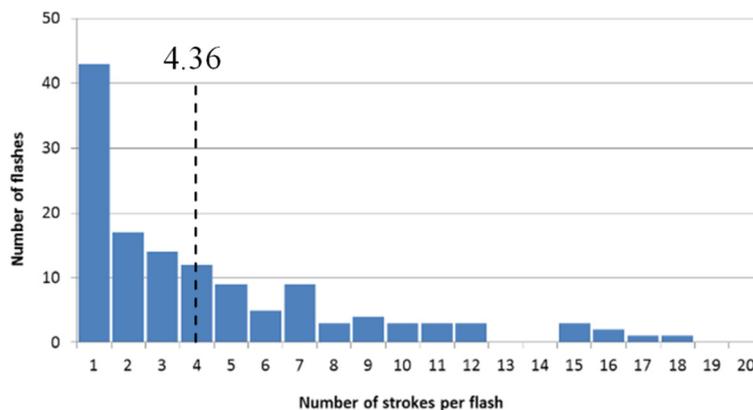

Fig. 3. Multiplicity of flashes around the Pic du Midi based on Météorage data.

2.3 Distribution related to the current intensity

As presented previously, the annual average number of strokes is 144 per year. Météorage estimate for each stroke detected the polarity and the current intensity. Thanks to this estimation, it is possible to plot the distribution of strokes over the period as a function of the current (see Fig. 4). Three important facts can be highlighted related to this distribution. Firstly, the polarity of all the strokes is negative. Secondly, most strokes have a current with a real value around 10 kA. Finally, the distribution shows the stroke number is negligible for currents either lower than 5 kA or larger than 40 kA. The absence of strokes with currents lower than 5 kA can be explained by the limited detection efficiency of the lightning location system for this range of currents. Indeed, Diendorfer [13] shows a decreasing of the detection efficiency at the Gaisberg tower for currents lower than 5 kA. The distribution in Fig. 4 can be approximated by a bi-exponential curve as:

$$N(I_p) = A \times \left[e^{\left(\frac{I_p - \Delta I_i}{k_1} \right)} - e^{\left(\frac{I_p - \Delta I_i}{k_2} \right)} \right] \times h\left[-\left(I_p - \Delta I_i \right) \right] \tag{1}$$

where A is the amplitude coefficient, I_p is the peak current value in kA, k_1 and k_2 are constants (in kA) controlling the front and the tail of the curve, ΔI_i represents a current offset and the function h is the Heaviside distribution. To match Eq. (1) with experimental data, the parameters are found by trial and error. The main criteria to determine this bi-exponential curve are both the minimization of the standard deviation and the conservation of the integral which must be equal to the total number of strokes (144 strokes per year). To simplify the analysis, the normalized distribution, shown in Fig. 5, is used throughout this paper, for which the coefficient A is calculated as $240/144 \approx 1.67$.

2.4 Calculation of upward flashes proportion

For the Pic du Midi site, with a tall antenna installed at the top of a mountain, the percentage of upward flashes (PUF) cannot be neglected because such structures are mainly struck by upward flashes [14]. Unfortunately, the information on PUF is not directly given by Météorage but two methods, described below, can be used to determine it.

2.4.1 Calculation based on the effective height

In the case of tall structures, it is usually considered that PUF depends on the structure height. PUF is negligible for structures lower than 100 m (approximately 13%) and reaches 100% for structures higher than 500 m. An expression for PUF based on experimental data is suggested by Rakov and Uman (paragraph 2.9.1. p50) [14] as:

$$\text{PUF} = 52.8 \times \ln(H_s) - 230 \tag{2}$$

where Hs is the structure height. Eq. (2) is valid for structures having the height between 78 m and 518 m. In the case of a structure located at the top of a mountain, the set can be approximated by an equivalent structure located on flat ground [15]. The height of this equivalent structure is termed 'effective' height. In order to estimate this effective height, the technique suggested by Zhou *et al.* [15] consists of approximating the mountain shape by a hemisphere. The Fig. 6 (provided by Google Earth) shows that on a 5 km × 5 km square area the average elevation around the Pic du Midi is about 2000 m. Consequently, the relative height of the Pic du Midi is about 900 m. Therefore, it has a real height of 3000 m, but it can be assimilated by a hemisphere of a 900 m relative height on a flat ground with the 100 m antenna mounted on top. The 900 m radius is the better value corresponding to the site profile. Moreover, a specific study has been performed for 400 m < He < 1000 m: there is no influence of this parameter on the resulting effective height. Without presenting details of calculations given by Zhou *et al.* [15], the effective height of the structure is obtained as 277 m.

Fig. 4. Annual stroke distribution at the Pic du Midi site, related to the stroke peak current
Red oscillatory line: experimental data; Blue smooth curve: Eq. (1), with parameters
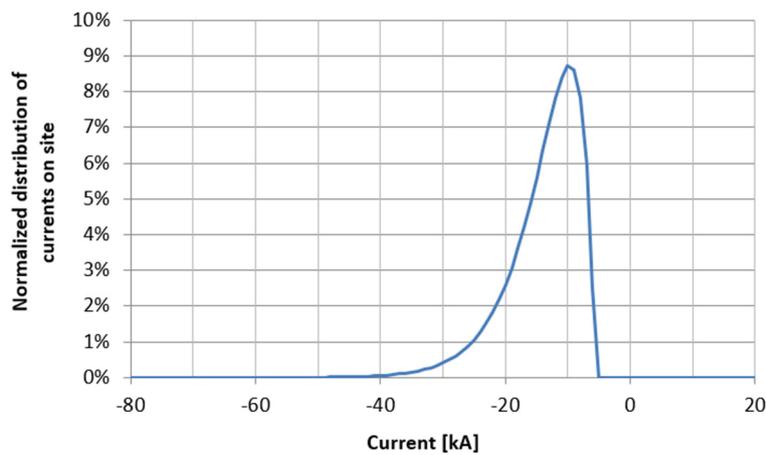indicated in the inset (according to Météorage data).

Fig. 5. Normalized stroke distribution at the Pic du Midi site, related to the stroke peak
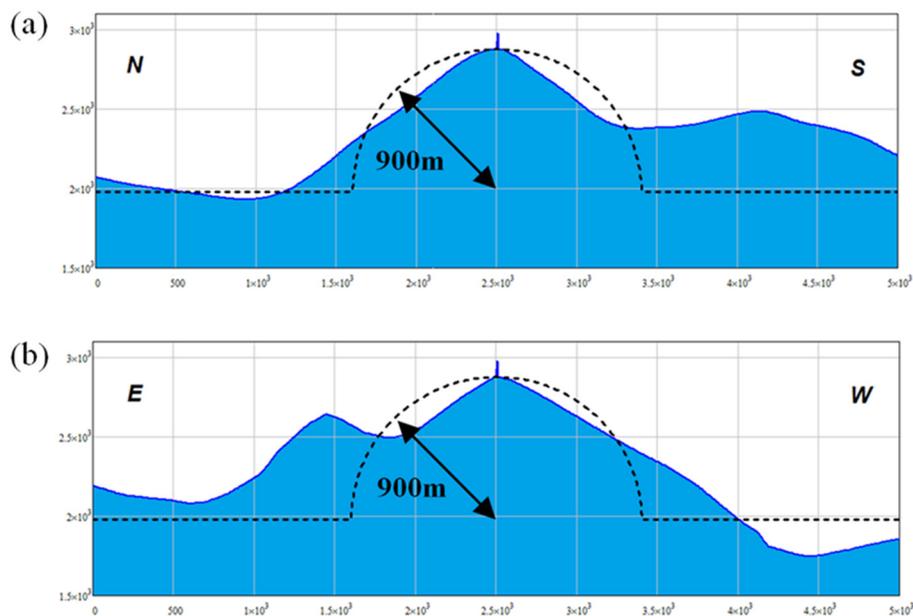current.

Fig. 6. Cross sections of the Pic du Midi mountain (a) along the North-South and (b) along
the East-West.

Consequently, by introducing this result in Eq. (2), the PUF is calculated as about 67%. It is important to note that the above approximation considers the mountain as an isolated entity located on a flat ground, like the Gaisberg mountain considered by Smorgonskiy *et al.* [16]. However, the Pic du Midi is actually surrounded by other relatively close mountains and these neighbors may induce secondary effects that can alter the effective height and correspondingly the PUF.

2.4.2 Calculation based on the analysis of network detection data

The second method for estimating PUF is applied in the case of the Gaisberg tower and the Mount San Salvatore [6]. The technique is applied in two stages. Firstly, for each site, two concentric circles are defined centered on the tall structure. The smaller circle has a radius of 1 km and represents the area where upward flashes are concentrated. The large circle with a radius of 8 km allows the calculation of the downward flash density, assumed to be homogeneous over the whole area.

Secondly, the total number of downward flashes in the small circle is simply obtained by multiplying the flash density with the area. The number of upward flashes is determined by subtracting the number of downward flashes to the total number of flashes. Then, the PUF can be calculated.

The same technique can be applied to determine the PUF for Pic du Midi. The analysis of data recorded by Météorage for a period of four years highlighted a number of 2640 strokes in a 10 km radius circle around the Pic du Midi (including the Pic du Midi) with 654 strokes on the Pic du Midi (1km radius circle area). Thus, the number of strokes in the 10 km radius circle without the Pic du Midi is 1986 strokes. So, the density is 6.4 strokes per km². As a consequence, in a 1 km radius, the corresponding annual number of downward strokes is 20. The percentage of downward strokes is obtained as 4%. We consider that an upward flash is composed by only upward strokes. The PUF is equal to the percentage of upward strokes and therefore the PUF is 96%. This value is consistent with the analysis performed by Watanabe [17] of data recorded at the Gaisberg tower whose the topography is similar to the Pic du Midi.

The two PUF values determined using the two techniques described above are quite different and therefore both will be considered separately below.

To conclude, the most important characteristics related to the lightning phenomena at the Pic du Midi site are:

· The strokes on the site are concentrated in a 500 m radius
· The multiplicity is 4.36 strokes per flash
· The strokes distribution as a function of the current presents a maximum at –10 kA
· The PUF is 67%, or 96%, depending on the technique used.

3. Evaluation of lightning impact probabilities

3.1. Basic description of a negative downward flash

The commonly accepted description of a negative downward flash is to consider that the negative charge at the base of the cloud induces an electric field between the cloud and the ground sufficiently important to initiate the development of a downward leader. Due to the leader propagation towards the ground, the electric field between cloud and ground is amplified. Approaching the ground, the electric field becomes so high that upward leaders can be generated from ground protrusions. This approach considers that the junction between the downward and upward leaders happens when the field reaches the critical value of 500 kV m^{-1} [18–20]. Corresponding to this moment, the distance between the downward leader tip and the ground is defined as the striking distance.

3.2. Electrogeometric model

The striking distance D (in m) is usually derived from experimental data using the following approximation [20]:

$$D = B \cdot I_p{}^b \qquad (3)$$

where I_p is the peak value of the lightning current of the first return stroke (in kA) and B and b are constants. The recommended values for these constants, by international standard of lightning protection IEC62305-1: 2006 [21], are $B = 10$ and $b = 0.65$.

For protecting structures against lightning, the electrogeometric model is considered using the rolling sphere method. This method is based on the two following assumptions:

- the equipotential surfaces around the leader tip are always spherical
- the striking distance is the same regardless of the nature and form of the ground structure.

Based on these assumptions, the impact points for each object of the structure at the striking distance D of the downward leader tip are determined as if the object is surrounded by an imaginary sphere of radius $r_s = $ D. In the case of a complex structure, such as a group of buildings, the method is applied by rolling the sphere on the structure profile (Fig. 7). All points of this structure in contact with the sphere may be stroked by lightning. On the other hand, objects not in contact with the sphere are considered protected against negative flashes having a current intensity larger than Ip. In terms of lightning protection, if the sphere comes into contact with a protective device without touching the objects, these objects are considered to be protected.
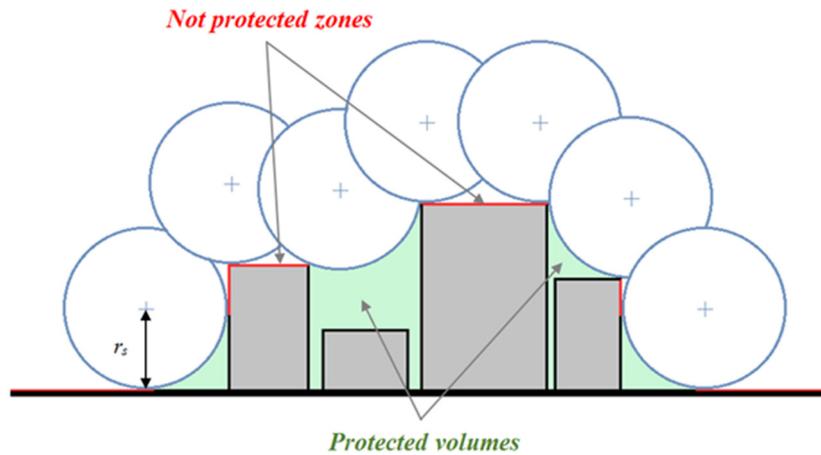

Fig. 7. Application of the rolling sphere method (of radius r_s) to a structure composed by different buildings.

3.3. Evaluation of lightning impact probabilities

The application of the rolling sphere method on a structure allows calculating a collecting effective area or the lightning impact probability on an aircraft using the area swept by the sphere center [4, 22]. The same methods will be considered below for the relatively complex profile of the observatory structure at the Pic du Midi de Bigorre. The aim is to highlight the areas that potentially can be struck by lightning and to evaluate their probability to be struck compared to the other parts of the structure.

In a 3-D problem, the surface swept by the sphere center is built by moving the rolling sphere over structure in the two horizontal directions. This surface (A_s) corresponds to the different positions of the negative leader tip which may attach to the structure just before the junction (Red points on Fig. 8 (a)). When the sphere is in contact with the structure, each point $C_s(i)$ of this surface corresponds to a position "i" of the rolling sphere center and for each sphere position "i", the contact points $\gamma_s(i)$ are associated with its center located at point $C_s(i)$. When the rolling sphere is moving on a flat portion of the structure (e.g. the ground or the plane roof of a building), a single position $C_s(i)$ of the center of the rolling sphere corresponds only to a single contact point $\gamma_s(i)$. In contrast, in the case of a prominent point (a lightning rod tip or a building corner), when the rolling sphere is moving the position of its center $C_s(i)$ turns around this point and draws a spherical portion $\alpha_s(i)$ around the same contact point $\gamma_s(i)$. Thus, for a given incremental step used to sweep the structure area, each contact point $\gamma_s(i)$ can be associated with a number $N_s(i)$ of different positions of the center of the sphere with which it is in contact. By normalizing $N_s(i)$ (corresponding to the partial surface $\alpha_s(i)$) associated to each contact points $\gamma_s(i)$ by the total number of points NTs forming the total surface As it is possible to establish an impact probability $P(i)$ for each contact point $\gamma_s(i)$ as:

$$P(i) = \frac{N_s(i)}{N_{Ts}} = \frac{\alpha_s(i)}{A_s} \tag{4}$$

In the case of the Fig. 8, the testing profile corresponds to a 3-D representation of a pyramid shape onto which the rolling sphere method is applied (Fig. 8 (a)). The sphere center trajectories Ts thus obtained are represented by the dotted area. The number $N_s(i)$ of rolling sphere center position associated with each profile point $\gamma_s(i)$ is shown in Fig. 8 (b). Therefore, it can be observed that the largest number of points associated (N_{smax}) corresponds to the top of the pyramid shape while a band around the base of the pyramid shape is not associated with any trajectory points. Indeed, the particular geometric profile implies the rolling sphere cannot be in contact with this band and therefore it directly corresponds to the protected volume.
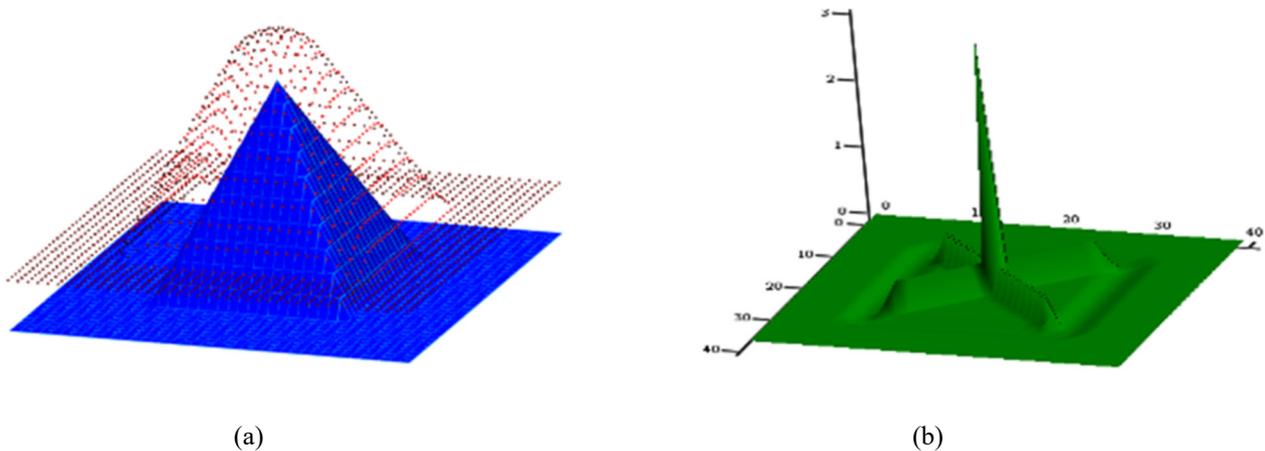

(a)   (b)

Fig. 8. Determination of impact probabilities from the rolling sphere method: application to a pyramid profile (a) Sphere center trajectory sweeping the profile (b) resulting probabilities.

4. Application to the Pic du Midi

4.1 Probabilities distribution

Once the lightning parameters on the Pic du Midi have been determined (see Section 2), the model described above can be applied. For this, an accurate 3-D representation of the site has been obtained (Fig. 9 (a)), made using a matrix of 520×250 cells with each cell corresponding to a 50 cm side square. Fig. 9 illustrates the results obtained by applying the rolling sphere method (presented in Section 3) to the profile of the Pic du Midi (Fig. 9 (a)) for a peak current value of -10 kA. A sphere, having the radius calculated using Eq. (3), provides the trajectory swept by its center (Fig. 9 (b)). Finally, from this trajectory, the impact probabilities are obtained for the entire site (Fig. 9 (c)). For each point of the studied structure, the method presented provides an impact probability related to the peak current. As expected, the probability distribution shown in Fig. 9 (c), exhibit two remarkable peaks: the largest corresponds to the probability of lightning impact on the TDF antenna while the next in order of magnitude corresponds to that on the lightning rod.

Fig. 10 gives the two probability distributions of these two structures for currents between -2 kA and -150 kA. They correspond to the impact probabilities on the top of the TDF antenna and on the tip of the lightning rod related to the current. It is important to note the fact that the probabilities are plotted for negative currents because the rolling sphere method based on the electrogeometric model is only defined for negative downward flashes. According to these distributions (Fig. 10), the impact probability on the TDF antenna and the lightning rod are just a few percentages for low current values i.e., 2.2% and 1.5% for a -2 kA current respectively. On the TDF antenna, the probability increases with the current and reaches almost 100% at -150 kA (triangles). In the lightning rod case, up to -40 kA, the probability also increases with current (squares). Beyond this value however, the probability decreases.

As a partial conclusion, for high current values, the major protuberances of the site constitute indeed a natural protection against lightning.
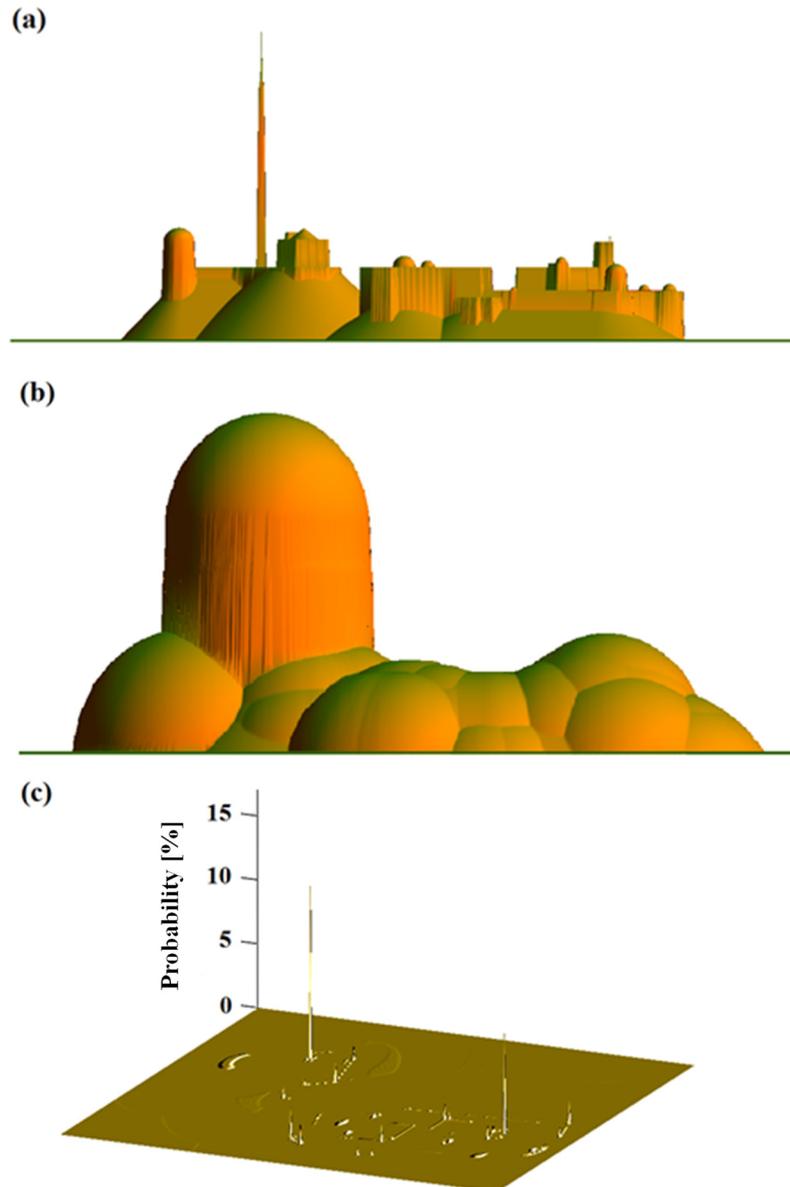
Fig. 9. Rolling sphere method application for Ip=10kA: (a) 3D representation of the Pic du Midi, (b) Surface swept by the moving sphere center, (c) resulting probability distribution.

4.2 Normalized probabilities

Fig. 10 application of the rolling sphere method provides an impact probability by negative downward flashes on two singular points of the site as a function of the current and in Fig. 5 is presented the normalized distribution of the flashes detected on the site and related to the current. By multiplying the value of these two distributions for each current value, the probability of the whole negative downward flashes on the two singular points as a function of the current can be obtained as shown in Fig. 11.

These two distributions highlight a maximum of probabilities at 10 kA (Fig. 11) while probabilities provided by the model around 10 kA are low (Fig. 10). Above 50 kA, the two distributions are near 0% (Fig. 11) while the sum of probabilities of the two singular points is almost 100% (Fig. 10). This is explained by the fact that the strokes observed on site are mostly around 10 kA and that those with a current higher than 50 kA are extremely rare. For instance, Fig. 5 shows that 8.7% of strokes on site have a magnitude of 10 kA while the percentage of 50 kA strokes is 0.0066% only. According to Fig. 10, the probabilities that a stroke hitting the TDF antenna has a current of 10 kA or 50 kA are respectively 10.9% and 71.8%. Therefore, multiplying these values gives the percentage of the strokes on site hitting the TDF antenna with a current of 10 kA or 50 kA: respectively 0.95% and 0.0047% (Fig. 11).
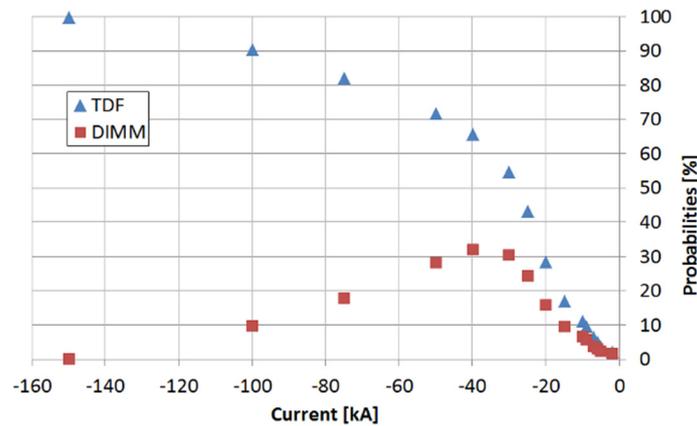
Fig. 10. Flashes probabilities distributions related to the current intensity on the TDF antenna and on the lightning rod.
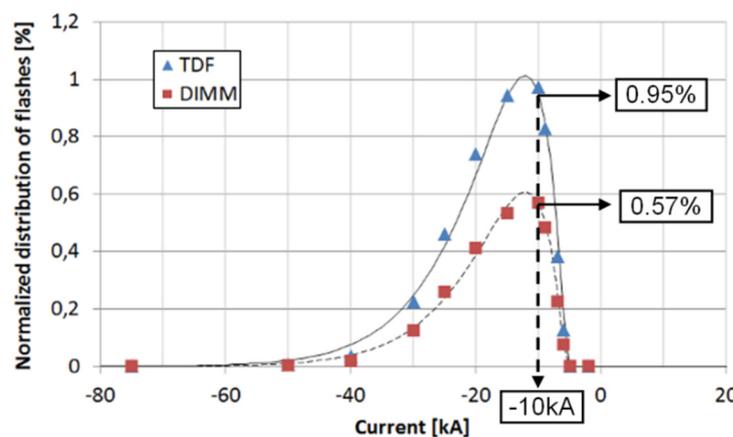

Fig. 11. Distribution of the whole negative downward flashes on the two singular points as a function of the current: on the TDF antenna and on the lightning rod.

In the same way as the distribution of the whole flashes on the site (related to the current) have been approximated (see Fig. 4), the new distributions can also be approximated by a bi-exponential curve based on Eq. (1) (black lines in Fig. 11) with the parameters of the two bi-exponential curves being presented in Table 1.

Table 1. Parameters of the two bi-exponential curves approximating the negative downward flashes distributions on the TDF antenna and the lightning rod of the DIMM platform.

	TDF antenna	DIMM platform
A	181	17
k_1 [kA]	606	6.6
k_2 [kA]	605	6.0
ΔI_i [kA]	−5.5	−5.7

This combined probability can provide the number of flashes which hit a point of the structure for a given current value. For example, for 100 downward flashes hitting the site, these curves predict that for 0.95 flashes will be with an intensity current of −10 kA on the TDF antenna and only 0.57 flashes will be with the same current value on the lightning rod. A very important result is obtained by calculating the integral of these bi-exponential curves providing the global probability on each point, a result independent of the current intensity. As a consequence, the probabilities for a negative downward flash to hit the two objects are:

· 18% for the TDF antenna
· 10% for the lightning rod

10

5. Calculation of the global probability and discussion

5. 1 Calculation of the global probability

Similar to the calculations presented in Section 2, the part of upward flashes on the Pic du Midi is 67% (or 96%, depending on the technique used) and it is considered that all will hit the TDF antenna. The remaining flashes are all downward and their distribution is related to the probabilities obtained with the method presented in Section 4 (i.e., 18% on the TDF antenna and 10% on the lightning rod). Coupling the results, by taking into account both the upward and downward flashes on the two particular objects, the global probabilities for flashes is obtained, independent of the type of discharges.

Finally, as discussed previously, Météorage detects 144 strokes average per year in a 500 m radius around the site. By considering the multiplicity, the number of strokes and flashes which can strike the TDF antenna and the lightning rod can be obtained. The final results, taking account both percentages of upward and downward flashes, are summarized in the Table 2 and Table 3. For example, Table 2 can be read as follow: from 33 flashes per year, 67% are upward flashes, all striking the TDF antenna, that is to say 22.1 flashes per year. The 10.9 flashes per year left are downward flashes and are distributed for 18% to the TDF (2.0 flashes per year) and 10% to the DIMM (1.1 flashes per year)

The calculations presented above focused on two particular objects: the TDF antenna and the lightning rod. However, probabilities can be deduced for all points of the Pic du Midi profile (Fig. 9 (a)) and for any place over the whole site.

5.2 Discussion

The lightning station installed at the top of the Pic du Midi mountain provides experimental data which can be compared to the results of present calculation [23]. During twelve months of recordings on site, only 17 flashes have been clearly recorded on the TDF antenna. This number seems to be low compared to the number predicted by the method presented i.e., 24.1 or 31.9 flashes per year depending on the technique (see Table 2 and Table 3). However, the site being often in fog, it is difficult to localize precisely all flashes hitting the Pic du Midi. In such conditions it is natural to assume the number of flashes on the TDF antenna higher which closes the gap between experimental data and theoretical predictions. In the case of the lightning rod of the DIMM platform, due to the low number of flashes, the experimental results are not accurately predicted by the theoretical model. During the last experimental campaign, no flash has been recorded on the DIMM platform, but three relatively deep grooves have been clearly observed on the lightning rod steel tip, which can only be produced by the interaction with a large current. These important findings show the number of flashes on the lightning rod is very low but definitely not zero, and in such conditions, the theoretical predictions i.e., 1.1 and 0.13 flashes (Table 2 and Table 3), are close to the experimental results.

Table 2. Summary of the probabilities considering a 67% proportion of upward flashes.

	Strokes yr^{-1}	Flashes yr^{-1}	Percentage
Pic du Midi	144	33	100%
TDF	105.1 (96.5 upward) (8.6 downward)	24.1 (22.1 upward) (2.0 downward)	73% (67% upward) (5.4 % downward)
DIMM	4.8	1.1	3.3%

Table 3. Summary of the probabilities considering a 96% proportion of upward flashes.

	Strokes yr^{-1}	Flashes yr^{-1}	Percentage
Pic du Midi	144	33	100%
TDF	139 (138 upward) (1.0 downward)	31.9 (31.7 upward) (0.2 downward)	96.5% (95.8% upward) (0.7% downward)
DIMM	0.58	0.13	0.4%

The PUF chosen (67% or 96%) corresponds to the following probabilities:
·　　73.0% or 96.5% on the TDF antenna,
·　　3.3% or 0.4% on the lightning rod.
It can be noticed that these results completely dependent on the upward and downward percentage chosen. Although until now no experimentally reliable value is available, the upward flashes percentage of 96% seems more suitable to be used in predictions. Indeed, at the Gaisberg and Pesseinberg towers having a topography similar to the Pic du Midi site, the downward flashes represent only 1% and consequently the percentage of upward flashes is 99% [6].

6. Conclusion

The evaluation of the lightning flash density is of crucial importance to the risk calculations, especially for the Lightning Protection Standards. The method presented in this paper allows calculating the impact probabilities on a structure. This method, based on the electrogeometric model application, considers several parameters such as the discharge type (downward or upward flashes), the flashes distribution as a function of the current or the multiplicity. The probabilities of lightning impacts on the Pic du Midi deduced indicate, as expected, that the largest probability corresponds to the TDF antenna. On the other hand, the calculations suggest for the impact probability on the lightning rod a very low value (but certainly not zero), in agreement with careful experimental observations on the site.

　　Future work can take into account other parameters, such as the emission of upward leaders in the case of a downward flash and Aït-Amar *et al*. suggested an improvement of the rolling sphere method by considering a cone at the top of protuberances to simulate such leaders [5].

　　The present model was applied to the Pic du Midi mountain, which is a very specific site (i.e., has a tall antenna, high altitude, etc.) where the percentage of upward flashes is large. These discharges are always detected with great difficulty by the lightning location system and future work aims to determine the percentage of upward and downward flashes more accurately on the site by using high-speed cameras and a more reliable current recording. Another future work will be dedicated to the application of the model to a site without a tall structure and therefore having a majority of downward flashes. It will be also interesting to validate the present model for various structure shapes, at different altitudes or in various climates.

Acknowledgment

References

[1]　Wagner, C. F., and Hileman, A. R., Mechanism of Breakdown of Laboratory Gaps, *Trans. AIEE. Part III: Power Apparatus and Systems*, Vol. 80 (3), pp. 604–618, 1961.
[2]　Armstrong, H. R., and Whitehead, E. R., Field and analytical studies of transmission line shielding, *IEEE Trans. Power Appar. Syst.*, Vol. PAS-87 (1), pp. 270–281, 1968.
[3]　Paris, L., and Cortina, R., Switching and lightning impulse discharge characteristics of large air gaps and long insulator strings, *IEEE Trans. Power Appar. Syst.*, Vol. PAS-87 (4), pp. 947–957, 1968.
[4]　Lalande, P., and Delannoy, A., Numerical methods for zoning computation, *AerospaceLab*, pp. 1–10: hal-01184414, 2012.
[5]　Ait-Amar, S., and Berger, G., A modified version of the rolling sphere method, *IEEE Trans. Dielecctr. Electr. Insul.*, Vol. 16 (3), pp. 718–725, 2009.
[6]　Smorgonskiy, A., Rachidi, F., Rubinstein, M., Diendorfer, G., and Schulz, W., On the proportion of upward flashes to lightning research towers, *Atmos. Res.*, Vol. 129–130, pp. 110–116, 2013.
[7]　Rakov, V. A., Uman, M. A., and Rambo, K. J., A review of ten years of triggered-lightning experiments at Camp

Blanding, Florida, *Atmos. Res*., Vol. 76 (1–4), pp. 503–517, 2005.

[8] Berger, G., Lafon, G., Serrie, G., and Pédeboy, S., New lightning experiment at the Pic du Midi, *International Conference on Lightning Protection (ICLP)*, Cagliari, Italy, Sep. 2010.

[9] Pédeboy, S., Identification of the multiple ground contacts flashes with lightning location systems, *CIGRE C4 Colloquium on Power Quality and Lightning*, Sarajevo, Bosnia and Herzegovina, May 2012.

[10] Schulz, W., and Diendorfer, G., Flash multiplicity and interstroke intervals in Austria, *International Conference on Lightning Protection (ICLP)*, Kanazawa, Japan, 2006.

[11] Pédeboy, S., Review of the lightning dataset and lightning locating systems performances as recommended by the IEC 62858 standard, *CIGRE C4 International Colloquium on Lightning and Power Systems*, Delft University of Technology, Netherlands, Oct. 2019.

[12] Diendorfer, G., Schulz, W., and Scherney, C., Areas of increased lightning flash density on mountain tops, *Lightning and mountains*, Chamonix, France, Jun. 1997.

[13] Diendorfer, G., LLS performance validation using lightning to towers, *Proc. 21st International Lightning Detection Conference*, Orlando, Florida, USA, 2010.

[14] Rakov, V. A., and Uman, M. A., Lightning: Physics and Effects. Cambridge University Press, 2007.

[15] Zhou, H., Theethayi, N., Diendorfer, G., Thottappillil, R., and Rakov, V. A., On estimation of the effective height of towers on mountaintops in lightning incidence studies, *J. Electrostat*., Vol. 68 (5), pp. 415–418, 2010.

[16] Smorgonskiy, A., Rachidi, F., Rubinstein, M., and Korovkin, N., On the evaluation of the effective height of towers: The case of the Gaisberg tower, *Proc. 31st International Conference on Lightning Protection (ICLP)*, Vienna, Austria, pp. 1–4., 2012.

[17] Watanabe, N., Nag, A., Diendorfer, G., Pichler, H., Schulz, W., Rakov, V., and Rassoul H.K., Characteristics of currents in upward lightning flashes initiated from the Gaisberg Tower, *IEEE Trans. Electromagn. Compat*., Vol. 61 (3), pp. 705–718, 2019.

[18] Gary, C., La foudre: des mythologies antiques à la recherche moderne. Masson, 1994. (*in French*)

[19] Gallimberti, I., Bacchiega, G., Bondiou-Clergerie, A. and Lalande, P., Fundamental processes in long air gap discharges, *C. R. Phys*., Vol. 3 (10), pp. 1335–1359, 2002.

[20] Uman, M. A., The art and science of lightning protection. Cambridge University Press, 2008.

[21] IEC 62305-1, Protection against lightning – Part 1: General principles, International Standard, 2006.

[22] Lalande, P., Etude des conditions de foudroiement d'une structure au sol, 1996. (*in French*)

[23] Sigogne, C., Pignolet, P., Reess, T., Berger, G., Lafon, G., and Serrie, G., New results at the Pic du Midi lightning station, *XII International Symposium on Lightning Protection (SIPDA)*, Belo Horizonte, Brazil, Jul. 2013.